Intrinsic vulnerability, hazard and risk mapping for karst aquifers: A case study

Article *in* Journal of Hydrology · January 2009

DOI: 10.1016/j.jhydrol.2008.11.008

2 authors:

Ziad Mimi
Birzeit University

Amjad Assi
Purdue University

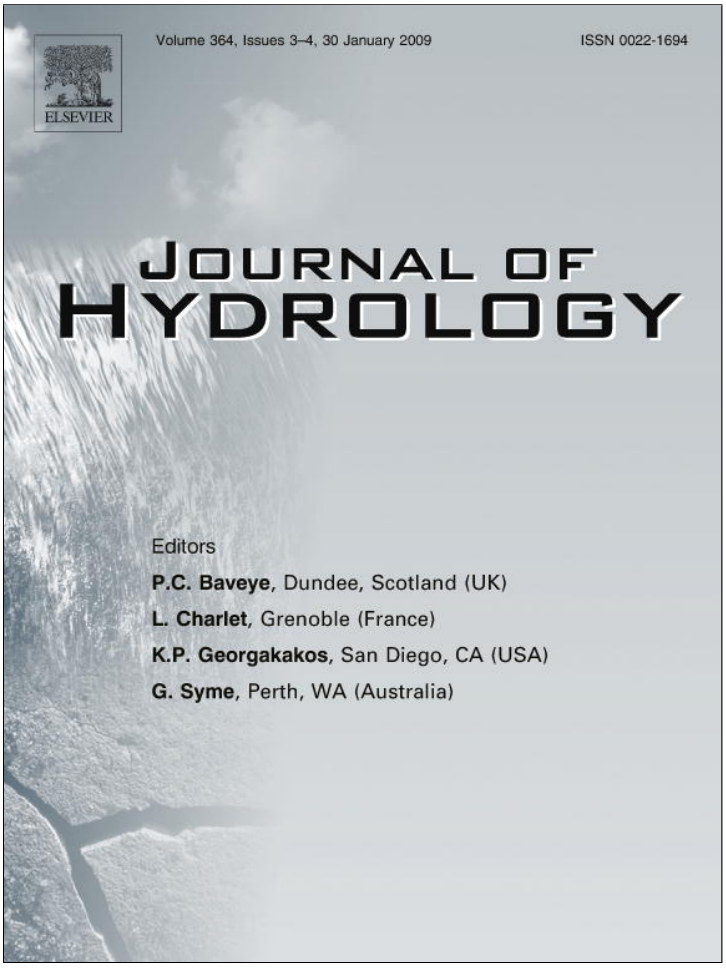
Volume 364, Issues 3–4, 30 January 2009
ISSN 0022-1694
ELSEVIER
JOURNAL OF
HYDROLOGY
Editors
P.C. Baveye, Dundee, Scotland (UK)
L. Charlet, Grenoble (France)
K.P. Georgakakos, San Diego, CA (USA)
G. Syme, Perth, WA (Australia)

Journal of Hydrology 364 (2009) 298–310

Contents lists available at ScienceDirect

Journal of Hydrology

journal homepage: www.elsevier.com/locate/jhydrol

Intrinsic vulnerability, hazard and risk mapping for karst aquifers: A case study

Ziad A. Mimi *, Amjad Assi

Institute of Environmental and Water Studies (IEWS), Birzeit University, P.O. Box 14, Birzeit, Palestine

ARTICLE INFO

Article history:
Received 25 April 2008
Received in revised form 22 October 2008
Accepted 6 November 2008

Keywords:
Intrinsic vulnerability mapping
Hazard vulnerability mapping
Risk vulnerability mapping
Karst aquifer
PI method
Palestine

SUMMARY

Groundwater from karst aquifers is among the most important resources of drinking water supply of the worldwide population. The European COST action 620 proposed a comprehensive approach to karst groundwater protection, comprising methods of intrinsic and specific vulnerability mapping, hazard and risk mapping. This paper presents the first application of all components of this European approach to the groundwater underlying the Ramallah district, a karst hydrogeology system in Palestine. The vulnerability maps which were developed can assist in the implementation of groundwater management strategies to prevent degradation of groundwater quality. Large areas in the case study area can be classified as low or very low risk area corresponding to the pollution sources due to the absence of hazards and also due to low vulnerabilities. These areas could consequently be interesting for future development as they are preferable in view of ground water protection.

Introduction

The emerging Palestinian state is located in southwest Asia on the eastern shore of the Mediterranean. It is composed of two separate areas, Gaza Strip and the West Bank. The eastern boundaries of the West Bank are the Jordan River and the Dead Sea, the western, northern and southern are Israel as shown in Fig. 1. There are two distinctive climatic seasons a wet winter and a dry summer. Annual average rainfall in the West Bank and Gaza is approximately 450 and 400 mm, respectively. The Jordan River system is the only surface water resource in the West Bank. There are two aquifers shared by Palestine and Israel: the Mountain Aquifer underlying the West Bank and the Coastal Aquifer underlying Gaza.

The present problems that are related to water are many and varied. Palestine, Israel, Jordan, and most other mid-eastern countries, which are generally characterized by aridity have very limited water resources. Future population projections in these countries place severe demands on already fragile reserves. Palestine will experience serious deficit and the shortage was estimated to be 271×10^6 m^3 for the year 2020 (Mimi et al., 2003).

Saving water, protection and augmentation of water supplies rather than development of new water resources and supply projects may prove to be in many cases the optimal policy. Cleaning and restoring groundwater is often technically problematic and costly, and finding alternative sources for water supply is not always possible. It is advisable also for environmental reasons to minimize leakage, to prevent pollution, and to reduce sensitivity to emergencies such as drought (Mimi et al., 2004).

Despite the important function of groundwater to the society, this resource has generally not been provided with adequate protection. The groundwater quality in Palestine is showing trends of increasing nitrate contamination, even if actual concentrations are below health standards. Combined with biological parameters and much anecdotal information, there are signs that health officials should be concerned about groundwater quality in public supplies, though hard evidence based on empirical data is largely absent (UNEP, 2003).

The majority of outcropping formations of the study area, Ramallah district, (Fig. 1) are the Lower Cenomanian and the Upper Cenomanian–Turonian complexes which are mainly composed of carbonate rocks such as limestone, dolomite, chalk and chert. Carbonate rock outcrops, of which a large part is karstified, cover the land surface (SUSMAQ, 2003b,2004b). Karst aquifers are particularly vulnerable to contamination: due to thin soils, flow concentration in the epikarst (the uppermost, often intensively fractured and karstified layer of a carbonate aquifer) and point recharge via swallow holes, contaminants can easily reach the groundwater, where they may be transported rapidly in karst conduits over large distances.

Hydraulic networks of carbonate rocks usually consisted of three types of spaces: pores, fissures, and caverns; sometimes filled forms also are present. At sufficiently large scales, the spaces are assumed to be homogeneous with arbitrary boundaries and to be characterized by mean values of parameters (Motyka, 1998).

Karstic aquifers are characterized by a dual porosity due to fractures and solutional voids (conduits) and frequently by a triple

* Corresponding author. Tel./fax: +970 2 2982120.
E-mail address: zmimi@birzeit.edu (Z.A. Mimi).

0022-1694/$ - see front matter © 2008 Elsevier B.V. All rights reserved.
doi:10.1016/j.jhydrol.2008.11.008

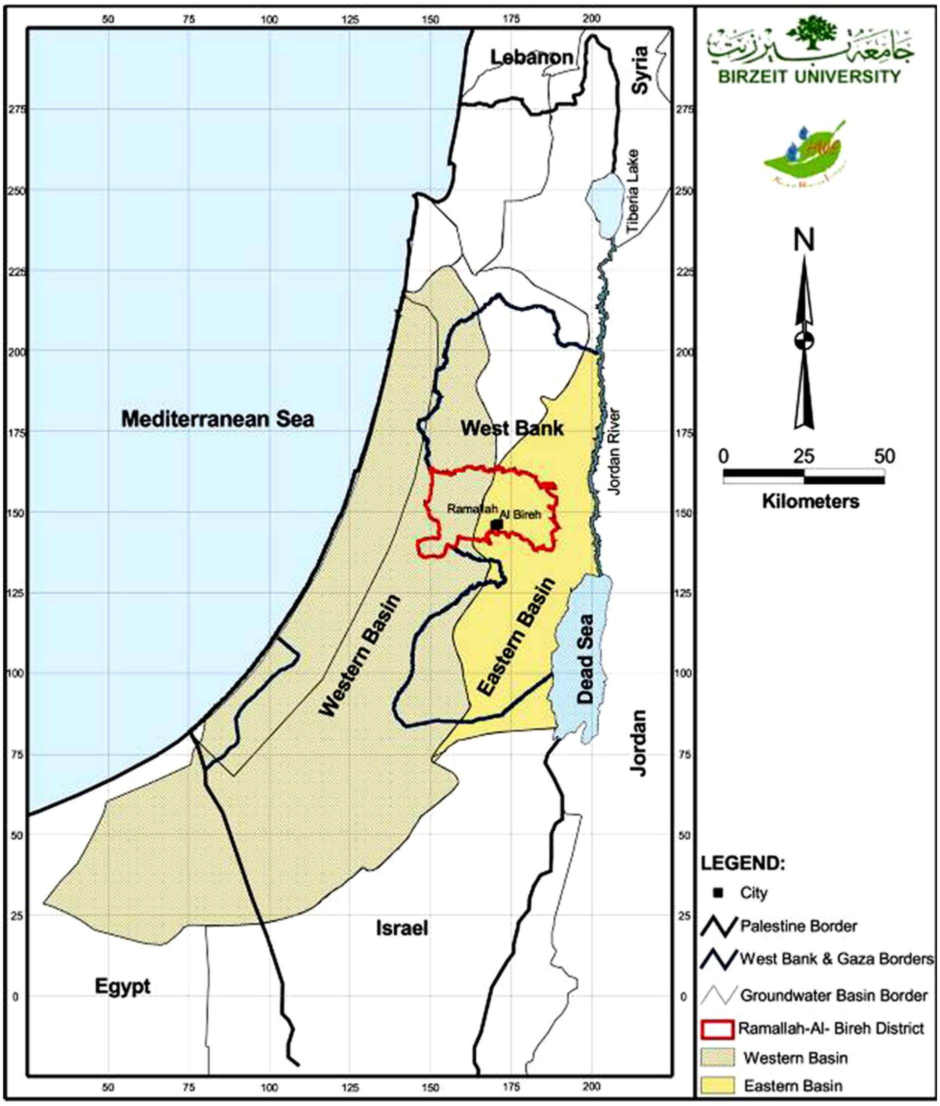

Figure 1. Location map for Ramallah district. (For interpretation of the references to colour in this figure legend, the reader is referred to the web version of this article.)

porosity due to the additional presence of intergranular pores (matrix). Groundwater storage takes place in the pores and fractures, while conduits act as drains. As there are both extremely fast and slow flow components within a karst system, contaminants can be transported very fast or stored for a very long time.

Karst aquifers are in need of particular attention constantly. Within the Karst system, it is vital at a minimum to protect the areas within a Karst system where contaminants can without much difficulty reach the groundwater. This takes us to the notion that a vulnerability of groundwater is not restricted to karst, but it is the most pertinent and the most complicated when applied to karst (Goldscheider, 2005).

The COST Action 620 on "vulnerability and risk mapping for the protection of carbonate (karst) aquifers" was set up by the European Commission's Directorate General for Science, Research and Development. Further impetus was given to the project by the European Water Framework Directive (2000), which is meant to provide a common framework for the policy and management of water resources. Within the framework of COST 620 new methods for intrinsic vulnerability, hazard and risk mapping were proposed (Zwahlen, 2003; Goldscheider, et al., 2000; Goldscheider, 2005).

From an application point of view, the maps are considered essential tools for both national and local entities with relevant responsibilities at the planning and decision-making level. At the consultancy level, applications appeared to be concerned mostly with the production of site-specific hazard and risk maps as an integral component of environmental impact studies (Rupert, 2001; Connell and Daele, 2003).

The aim of this paper is to present intrinsic vulnerability, hazard and risk mapping for the aquifers underlying Ramallah district, West Bank and Palestine. One of the aims of this research is the application, for the first time in Palestine, of the intrinsic vulnerability, hazard and risk mapping that could serve as a non-subjective mathematical tool for a rational management of groundwater resources and subsequent land use planning.

Intrinsic vulnerability mapping

Several methods exist for intrinsic vulnerability mapping of groundwater. Among the most commonly known are DRASTIC (Aller et al., 1985) and GOD (Foster, 1987). There have been reviews of several existing methods by Vrba and Zaporozec (1994), COST 65 (1995), Gogu and Dassargues (2000), and Goldscheider (2002). A new method for mapping vulnerability, within the framework of COST 620 was put forth: the PI method. PI stands for the two factors that are taken into consideration: protective cover (*P*) and the infiltration conditions (*I*). (Goldscheider et al., 2000). The PI method can be applied to all types of aquifers, though provides special methodological tools for karst. It is based on an origin-pathway-target model. The term 'origin' is used to depict the location of a potential contaminant release. The 'pathway' involves the passage of potential contaminants from the point of release to the 'target'.

The detailed assessment schemes for the *P* and *I* factors can be found in Goldscheider et al. (2000), Goldscheider (2002,2005) and in the final report of the European COST Action 620 (Zwahlen, 2003). The following paragraphs, therefore, give a brief description only.

The protective function of all layers that may be present in the vadose zone is described by the *P* factor: the topsoil, the subsoil, the non-karst rock and the unsaturated zone of the karst rock. The protectiveness can be assessed on the basis of the effective field capacity (eFC) of the soil, the grain size distribution of the subsoil, the lithology, fissuring and karstification of the non-karst and karst rock, the thickness of all strata, the mean annual recharge and Artesian pressure in the aquifer. The total score range is composed of five classes, from $P = 1$ for an extremely low degree of protection to $P = 5$ for very thick and protective overlying layers. The *P* map shows the distribution of the *P* factor.

The *I* factor describes the infiltration conditions and, in particular, the degree to which the protective cover is bypassed as a result of lateral surface and subsurface flow that enters the karst aquifer at another place. The factor's values range between 0.0 and 1.0. Its value is 1.0 on a horizontal, highly permeable soil where all recharge will occur in a diffuse way. The *I* factor is 0.0 on a steep slope made of low permeability soil that focuses surface runoff towards a sinking stream. The protective cover will be completely bypassed in such a situation. All other areas are assigned intermediate values (0.2, 0.4, 0.6 and 0.8), depending on the soil properties controlling the predominant flow process, the vegetation and slope gradient, and the position of a given point inside or outside the catchment of a sinking stream (Goldscheider, 2005).

The product of *P* and *I* which is π is the final protection factor. Five classes of vulnerability (or protectiveness) are distinguished and symbolised by colours ranging from red to blue, as proposed by Vrba and Zaporozec (1994). A protective factor of $\pi \leqslant 1$ indicates a very low degree of protection and an extreme vulnerability to contamination, symbolised by a red colour. A value of $\pi = 5$ means a very low vulnerability and a very high degree of protection, symbolised by a blue colour. The vulnerability map shows the distribution of the π factor. The *P* map and *I* map legend is comprised of five colours from red to blue as Table 1 shows (Goldscheider, 2005).

Hazard mapping

The following summarize the steps for hazard mapping (Zwahlen, 2003):

Step 1: Definition and inventory of hazards

In the context of groundwater contamination, a hazard is defined as a potential source of contamination resulting from human activities taking place mainly at the land surface. A hazard assessment considers the potential degree of harmfulness for each type of hazard. It is determined by both the toxicity and the quantity of harmful substances, which may be released as a result of a contamination event. It is proposed that the hazards should be classified according to the type of land use. A general differentiation of the land use on a local or regional scale distinguishes between three main categories, i.e. infrastructural, industrial and agricultural activities. These main categories are proposed as Level I categories of hazards in the hazard inventory.

The proposed Level II categories distinguish between hazards according to the main source (solid or liquid contaminants) of possible groundwater contamination, or else refer to types of industrial or agricultural activities with their corresponding spectrum of possible pollutants. A further subdivision into Level III categories with their weighting values is shown in Table 2 (as an example). Cost 620 presented a detailed table for most of the hazards that may exist in any area with their weighting values.

Step 2: Hazard data requirements

Assessing the potential degree of harmfulness for each type of hazard requires information on the following: process or nature of activity, type of harmful substances, amount of substances which can be released and age and status of installations and plants. The information to be collected for each type of hazard

Table 1
Common legend for the vulnerability map, the *P* and the *I* map.

	Vulnerability map vulnerability of ground water		*P-Map* protective function of overlaying layers		*I-Map* degree of bypassing	
	Description	π-Factor	Description	*P* Factor	Description	*I* Factor
red	Extreme	0–1	Very low	1	Very high	0.0–0.2
orange	High	>1–2	Low	2	High	0.4
yellow	Moderate	>2–3	Moderate	3	Moderate	0.6
green	Low	>3–4	High	4	Low	0.8
blue	Very low	>4–5	Very low	5	Very low	1.0

Table 2
Hazard weighting values for some hazards as an example.

No.	Hazards	Weighting value
1	Infrastructural development	
1.1	Waste water	
	Urbanization(leaking sewer pipes and sewer systems)	35
	Urbanization without sewer systems	70
	Detached houses without sewer systems	45
	Septic tank, cesspool, latrine	45
	Runoff from paved surfaces	25
	Waste water discharge into surface water course	45
1.2	Municipal waste	
	Garbage dump, rubbish bin, litter bin	40
	Waste loading station and scrap yard	40
	Sanitary landfill	50
	Spoils and building rubble depository	35
	Sludge from treatment plants	35
1.3	Fuels	
	Storage tank, above ground	50
	Storage tank, underground	55
1.4	Transport and traffic	
	Road, unsecured	40
	Road tunnel, unsecured	40
1.5	Recreational facilities	
	Tourist urbanization	30
1.6	Diverse hazards	
	Animal burial	35
2	Industrial activities	
2.1	Mining (in operation and abandoned)	
	Mining of salt	60
2.2	Excavation sites	
	Excavation and embankment for development	10
	Gravel and sand pit	30
2.3	Oil and gas exploitation	
	Production wells	40
	Reinjection wells	70
	Loading station	55
2.4	Industrial plants (none mining)	
	Iron and steel works	40
	Chemical factory	65
	Leather tannery	70
	Food industry	45
2.5	Power plants	
	Gasworks	60
2.6	Industrial storage	
	Stock piles of raw materials and chemical	60
	Containers for hazardous substances	70
2.7	Diverting and treatment for waste water	
	Waster water pipelines	65
	Surface impoundment for industrial waste water	65
	Discharge of treatment plants	40
3	Livestock and Agriculture	
3.1	Livestock	
	Animal barn	30
	Factory farm	30
3.2	Agriculture	
	Open silage (field)	25
	Stockpiles of fertilizers and pesticides	40

should be grouped according to the following criteria: identification of the nature of the activity, localization of the activity by topographic coordinates, characterization and quantification of the solid and liquid waste production.

Step 3: Rating and weighting of hazards

Table 2 determines the weighting coefficient or the "harmfulness of a hazard to groundwater (H)". The weighting values listed in Table 2 vary between 10 and 100. For a comparison between hazards of the same type, all the different factors influencing the degree of harmfulness have to be considered. According to the general definition of the hazard categories, the hazardous substances involved within each individual category are more or less the same or can be considered to be from the same group. Therefore the differences in harmfulness within each hazard category will be mainly due to the variable quantity (Q_n) of harmful substances, which can be released and further seep into the underground. It is recommended that these weighting values should be changed only slightly by multiplying them with a ranking factor between 0.8 and 1.2 in order to indicate low or high amounts, respectively, of toxic substances compared with the general average.

To avoid time consuming work a reduction factor R_f is recommended. This coefficient provides an assessment of the probability for a contamination event to occur. If no information on the above mentioned factors is available, then $R_f = 1$. Otherwise, positive information concerning the reduction of the likelihood can be used to reduce the hazard index. The hazard index (HI) describes the degree of harmfulness of each hazard. For its calculation the Eq. (1) is recommended:

$$\mathrm{HI} = H^{*}Q_{n}^{*}R_{f} \tag{1}$$

whereby HI is the hazard index, H is the weighting value of each hazard as assigned in Table 2, Q_n is the ranking factor (0.8–1.2) and R_f the reduction factor (0.0–1.0). The possible range of the hazard index HI runs from 0 to 120 scores.

Step 4: Production of hazard map

The graphical interpretation of hazard data is obtained from a map, which shows spatial information such as their location and extent (size, shape), together with descriptive information, which are the map features or attributes. The mapping can be performed using a Geographic Information System (GIS). As shown in Table 3, the colours representing the potential degree of harmfulness of the different hazards are assigned according to the resulting hazard index.

Risk mapping

Morris and Foster (2000) defined groundwater pollution risk "as the probability that groundwater in the aquifer will become contaminated to an unacceptable level by activities on the immediately overlying land-surface". This approach uses the interaction between the subsurface contaminant load and the aquifer

Table 3
Hazard Index and Hazard Index classes.

Hazard index	Hazard index class	Hazard level	Colour
0–24	1	No or very low	Blue
>24–48	2	Low	Green
>48–72	3	Moderate	Yellow
>72–96	4	High	Orange
>96–120	5	Very high	Red

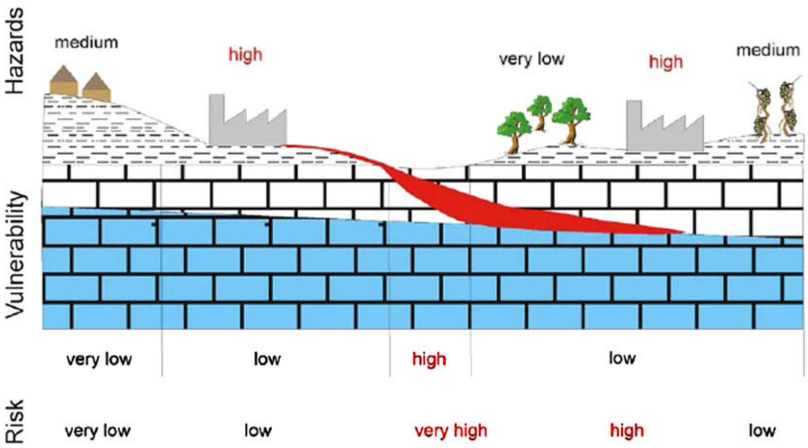

Figure 2. Risk assessment of groundwater considering only the superimposed effects of hazards and vulnerability. (For interpretation of the references to colour in this figure legend, the reader is referred to the web version of this article.)

Table 4
Classification of the risk map.

π-Factor	Hazard index	1/HI	$\pi\cdot(1/H)$	Risk class	Risk level	Colour
4–5	0–24	>0.042	>0.167	1	No or very low	Blue
3–4	24–48	0.042–0.021	0.067–0.063	2	Low	Green
2–3	48–72	0.021–0.014	0.063–0.028	3	Moderate	Yellow
1–2	72–96	0.014–0.010	0.028–0.010	4	High	Orange
0–1	96–120	<0.010	<0.010	5	Very high	Red

pollution vulnerability at the location concerned described as "risk intensity assessment". The approach is frequently used, as it is a rather simple way to assess the risk intensity. These maps show the risk of groundwater pollution of each hazard in relation to resource protection. The decisive risk index is the probability that contaminants with a certain amount and concentration (risk intensity index) reach the surface of the groundwater. The calculation of the risk intensity index considers the effects of the intrinsic vulnerability and the hazard by using (Zwahlen, 2003)

$$RII = 1/HI \cdot \pi \tag{2}$$

where RII is the risk intensity index, HI is hazard index and π is PI factor (index for intrinsic vulnerability).

Fig. 2 illustrates the various possible interactions of the hazard and vulnerability distribution on risk intensity assessment. The Risk Intensity Index for groundwater contamination depends not only on vulnerability but also on the existence of significant pollutant loading entering the subsurface environment. It is possible to have high aquifer vulnerability but low risk index, if there is no significant pollutant loading; and conversely to have a high risk index value in spite of low vulnerability, if the pollutant loading is exceptional or if there is the possibility of bypassing in less vulnerable areas (Zwahlen, 2003).

The limits of the risk classes are the product of the limits of the vulnerability classes and the Hazard Index (Table 4), an operation that is very easy to implement with other vulnerability methods.

Description of the case study area: Ramallah district

The groundwater resources of Palestine are abstracted from aquifers extending from the West Bank to Israel. The main aquifer basins in the West Bank are the eastern, northeastern and western basins. Ramallah district lies over the eastern and western basins (Fig. 1). However, the majority of outcropping formations in Ramallah district are the lower Cenomanian and the Upper Cenomanian–Turonian complexes which are mainly composed of carbonate rocks such as limestone, dolomite, chalk and chert.

The western mountain basin underlies about 45% of Ramallah district and its water flows towards the west. It extends from the Judean desert northward to the Carmel mountain foothills, and from near the center of the mountain belt westward to the coastal plain. The basin is underlain by a thick sequence of layered limestone, dolomite, chert, chalk, and marls which form the upper and lower aquifers. It is overlain by Senonian chalks of the Eocenian age. The upper and lower aquifers are of upper Albian and upper Cenomanian–Turonian age, respectively. Lower Cenomanian sequences with higher amounts of marl divide the two aquifers. Over a small percentage of the area in the west, these units are overlain by younger Neogene and Pleistocene formations consisting of sand, gravel, and conglomerate. The Quaternary series are referred to as Kukar group (Rofe and Raffety, 1963; Shachnai, 1969; Braun, 1972; Arkin, 1980; SUSMAQ, 2003a).

The eastern mountain basin underlies the eastern part of Ramallah district and the western part of Jericho district. It includes the eastern part of the mountain belt and the steep western Escarpment of the Jordan Rift Valley. The Jordan Rift Valley forms the eastern boundary of the basin. Annually renewable groundwater from natural rain infiltration forms the principal source of freshwater in the basin and is supplied to wells and springs by three principal aquifers: the Turonian aquifer, the upper Cenomanian aquifer and the lower Cenomanian aquifer. (Rofe and Raffety, 1963; Shachnai, 1969; Braun, 1972; Arkin, 1980; SUSMAQ, 2003a).

Intrinsic vulnerability mapping

*Determination of the **P factor***

The *P* factor takes into account the effectiveness of the protective cover as a function of the thickness and hydraulic properties of all the strata between the ground surface and the groundwater surface. *P* factors for the case study area will be shown on the *P* map. The following is the detailed analysis for the study area.

Top soil and subsoil

There are different types of top soils and sub soils in the study area as shown in Fig. 3. *T-value* for top soil and *S-value* for subsoil were determined based on the characteristics of these types as shown in Table 5 (SUSMAQ, 2003a,2004a). The soil map was converted to a grid map by using Arc-View software. In the grid map, each cell has its own *T*-value. For each sub-soil type, the thickness (*M*) was estimated. Then, the soil map was converted into a grid map where each cell has its own SM-value.

Lithology and fracturing

The lithology (*L*) is the physical makeup, including the mineral composition, grain size, and grain packing, of the sediments or rocks that make up the geological system. While fracture (*F*) is a natural phenomenon which occurs in rocks and causes separation into pieces under the action of stress. However the Bedrock (*B*) is the multiplication between the two values *L*-value and *F*-value.

Table 6 presents the two values (*L*-value and *F*-value) for the case study area. The values were calculated based on the geological map (Fig. 4), SUSMAQ(2003a,2004a). The Bedrock (*B*) shown in the last column of the table is the multiplication between the two values (*L*-value and *F*-value).

The thickness of each stratum in meters (*M*) was estimated using the stratigraphical section of the West Bank and was multiplied by *B*. The geology map was converted into a grid map where each cell has its own BM-value. The value of (*A*) was determined based on the outcropping formations. If the aquifer is confined, then *A* = 1500 otherwise *A* = 0.

Recharge

Recharge values were determined based on rainfall–recharge equations adopted from SUSMAQ (2004a). These equations were applied depending on outcropping formations in the study area. When the geological formations that form the main aquifers are outcropping, the following rainfall–recharge equations are applied. Fig. 5 presents the recharge (mm/y) while Table 7 presents the recharge (mm/y) and recharge value. The recharge map was converted into a grid map where each cell has its own *R*-value.

$$R = 0.6(P - 285) \quad P > 700\ \text{mm}$$
$$R = 0.46(P - 159) \quad 700\ \text{mm} > P > 456\ \text{mm}$$
$$R = 0.3(P) \quad 456\ \text{mm} > P$$

where *R* is the recharge from rainfall in mm/y and *P* is annual rainfall in mm/y.

Based on Fig. 5, Eq. (3) below and Table 8, the Total protective function (P_{TS}) for each cell was calculated. Accordingly, the *P* map was prepared as shown in Fig. 6. It was found that about 5 km^2 (0.6% of total area) is classified as moderate protective,

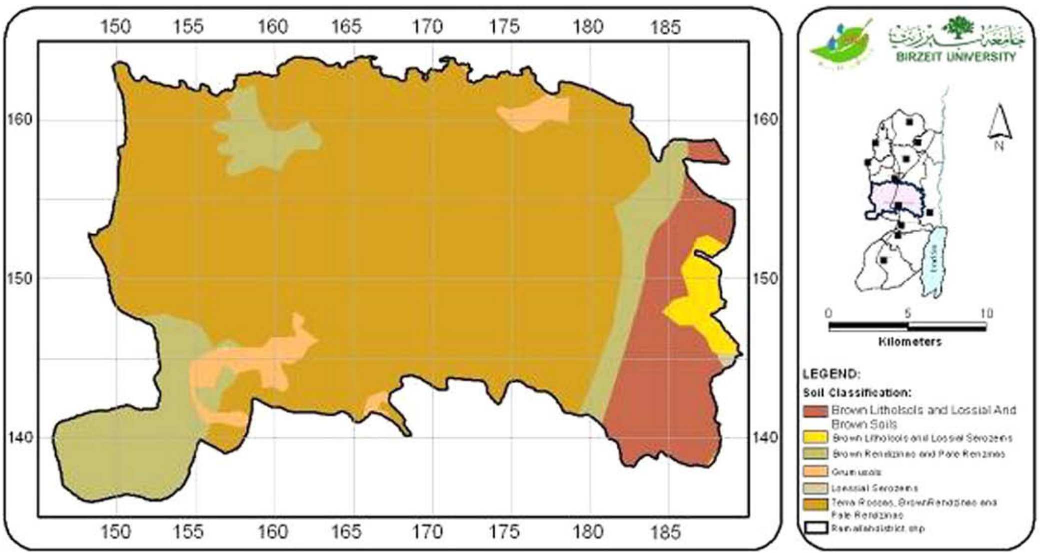

Figure 3. Soil types distribution for Ramallah district. (For interpretation of the references to colour in this figure legend, the reader is referred to the web version of this article.)

Table 5
T- and *S*-values for top soils and sub-soils.

Top soil type	Sub-soil type	Effective field capacity (eFC) (mm)	*T*-Value	*S*-Value
Terra Rossa, Brown Rendzinas and pale Rendzinas	Clay	446	750	500
Brown Rendzinas and pale Rendzinas	Clayey loam	334	750	300
Grumusols	Clay	460	750	500
Brown Lithosols and Loessial Serozems	Silty clayey sand	90–140	125	75
Brown Lithosols and Loessial Arid Brown Soil	Loamy	140–200	250	250
Loessial Serozems	Silty clay	140–200	250	320

Table 6
Lithology and fracturing values for unsaturated layers.

No	Lithology	Hydro-stratigraphy	Lithology value (L)	Fracturing value (F)	$B = L \times F$
1	Nari (surface crust) and alluvium gravels and fan deposits	Local aquifer	5	4	20
2	Thinly laminated marl with gypsum bands and poorly sorted gravel and pebbles	Aquitard	10	10	100
3	Conglomerates, marl, chalk, clay and limestone	Local aquifer	5	20	100
4	Nummulitic reefal limestone	Aquifer	5	1	5
	Nummulitic bedded limestone		5	1	5
	Nummulitic limestone, chalk		10	10	100
	Chalk, Nummulitic limestone		10	10	100
5	Marl, Chalk	Aquitard	20	25	500
	Chalk, Marl		20	25	500
6	Main Chert, Phosphate	Aquiclude	15	15	225
	Chalk and Chert		15	15	225
7	White limestone, stilolithes	Upper aquifer	5	1	5
	Limestone and Dolomite		5	0.5	2.5
	Yellow thin bedded limestone		5	1	5
	Dolomite, soft		5	0.3	1.5
	Chalky limestone, Chalk		12	4	36
	Karstic Dolomite		5	0.3	1.5
	Yellow Marl		20	25	500
	Lime & Dolostone, Chalk, (Clay)		20	20	400
8	Reefal Limestone Dolomite Limestone, interbedded with Marl	Lower aquifer	5	1	5
	Dolomite		8	8	64
	Karstic Limestone		5	0.3	1.5
	Marl, marly nodular limestone		5	0.1	0.5
	Marly limestone and limestone		20	10	200
			20	10	200

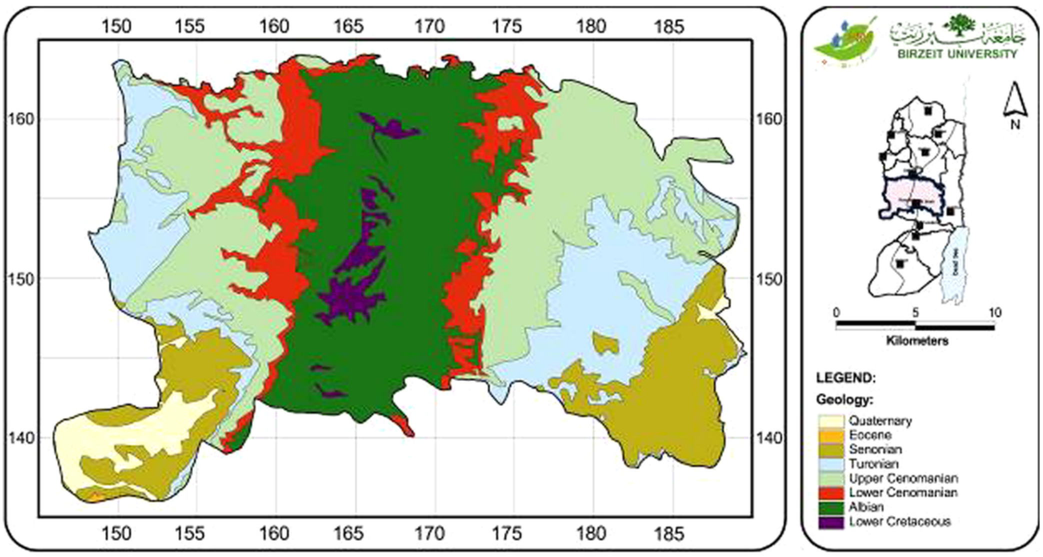

Figure 4. Geological map for Ramallah district. (For interpretation of the references to colour in this figure legend, the reader is referred to the web version of this article.)

and 637 km^2 (76.7% of total area) is high protective whereas 189 km^2 (22.7% of total area) is very high protective areas.

$$P_{TS} = \left[T + \left\langle \sum_{i=1}^{m} S_i.M_i + \sum_{j=1}^{n} B_j.M_j \right\rangle .R + A\right] \quad (3)$$

where P_{TS} is the total protective function, T is top soil, S is subsoil, M is thickness of each stratum (m), B is bedrock = $L^* F$, L is lithology, F is fracturing, R is recharge and A is Artesian pressure.

Determination of the *I factor*

The I factor shows the degree to which the protective cover is bypassed by lateral surface and subsurface flow and subsequent concentrated recharge. The following three steps were carried out in order to determine the I factor and construct the I map, respectively.

Determination of the dominant flow process

The dominant flow process is assessed on the basis of the topsoil permeability and the presence permeability soils. Subsurface flow takes place in highly permeable soils with low permeability layers, while infiltration predominates if low permeability layers are absent. The digital soil map contains data on the permeability of the soils in different depths (0–30, 30–60, 60–100 cm) and the underlying bedrock. The dominant flow process was determined by intersecting the coverage ‘topsoil permeability’ and ‘depth to low permeability layers’.

Flow Process is a function of the saturated hydraulic conductivity (HC) (m/s) and the depths to low permeability layers where

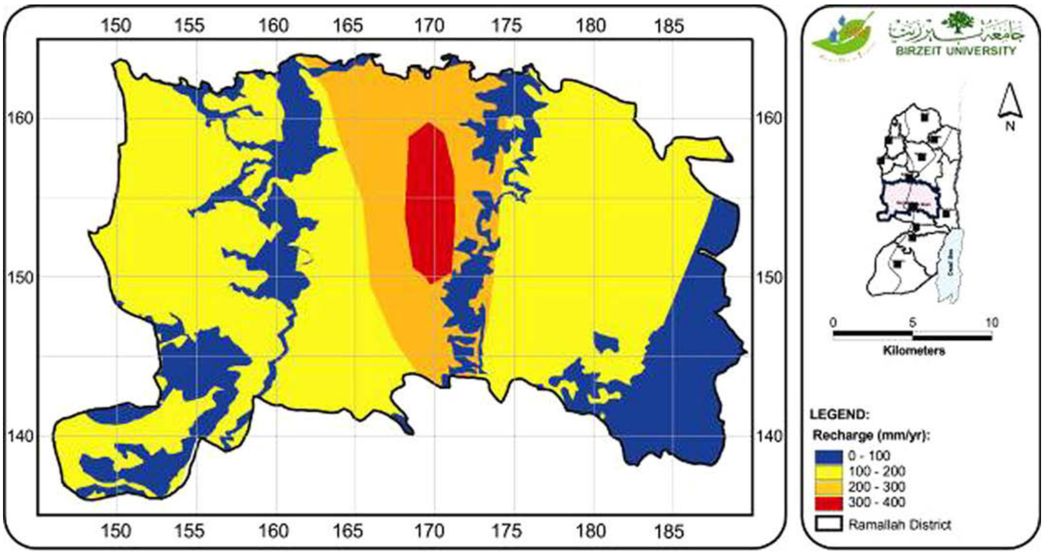

Figure 5. Recharge for Ramallah district (mm/yr). (For interpretation of the references to colour in this figure legend, the reader is referred to the web version of this article.)

Table 7
Groundwater recharge estimation for different mean annual rainfall and corresponding recharge values (R).

Mean annual rainfall (mm)	Recharge (mm/y)	R-value
200–250	60–75	1.75
250–300	75–90	1.75
300–350	90–100	1.75
350–400	105–120	1.5
400–450	120–135	1.5
450–500	135–157	1.5
500–550	157–180	1.5
550–600	180–200	1.5
600–700	200–250	1.25
700–1000	250–430	1.00

hydraulic conductivity means the ease with which water passes through soil. For Ramallah district the hydraulic conductivity for Terra Rossa is 2.78×10^{-7} m/s, for Brown Rendzinas it is 1.67×10^{-6} m/s, and for Grumusols it is 6.94×10^{-8} m/s (SUSMAQ, 2003a, 2004a). The dominant flows for different soil types have been estimated and presented in Table 9 and Fig. 7.

Table 8
Relation between total protective function (P_{TS}) and P-factor.

P_{TS}	Effectiveness of protective cover	P Factor
0–10	Very low	1
>1–100	Low	2
>100–1000	Medium	3
>1000–10,000	High	4
>10,000	Very high	5

Determination of the I′ factor

The intensity of lateral surface and subsurface flow also depends on the slope gradient and the vegetation/land use. Gentle slopes and forests favour infiltration, while steep slopes and agricultural land use favour lateral flow. The I' factor is determined

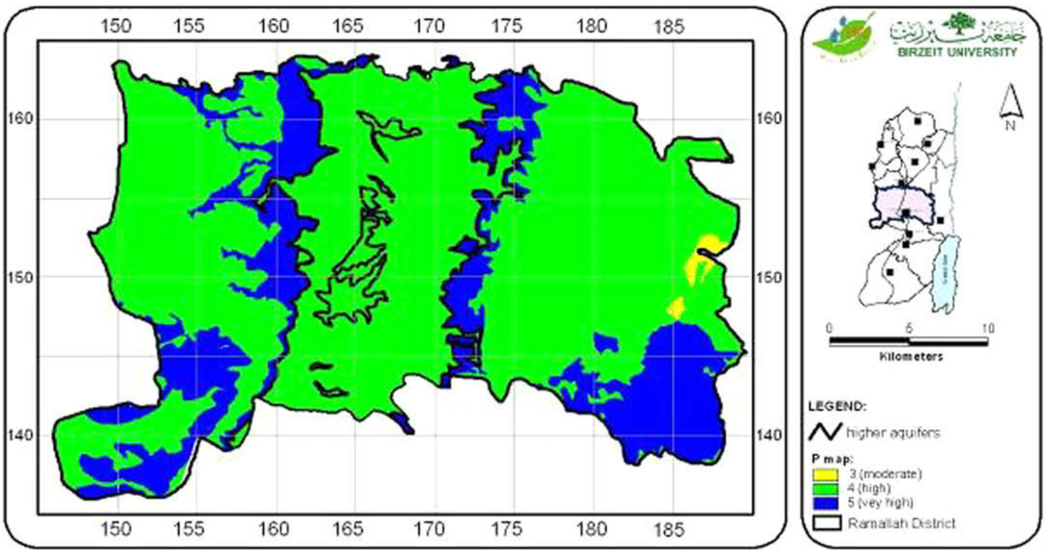

Figure 6. Protective cover map (P-map). (For interpretation of the references to colour in this figure legend, the reader is referred to the web version of this article.)

Table 9
Dominant flow for different soil types for Ramallah district.

Soil type	Dominant flow	Flow type
Terra Rossa, Brown Rendzinas and Pale Rendzinas	Hortonian surface flow	F
Brown Rendzinas and Pale Rendzinas	Infiltration and subsequent percolations	A
Grumusols	Hortonian surface flow	F
Brown Lithosols and Loessial Serozems	Saturated surface flow	D
Brown Lithosols and Loessial Arid Brown Soil	Saturated surface flow	D
Loessial Serozems	Saturated surface flow	D

by intersecting the coverages ‘dominant flow process’, ‘vegetation’ and ‘slope gradient’.

Based on the flow type (first step), slope topography map, land use map (Fig. 8), I' map was constructed as shown in Table 10 and Fig. 9.

Determination of the I factor

Lateral surface and subsurface flow is relevant for groundwater vulnerability only if the water enters the underground at another place. Consequently, the *I* map presented in Fig. 11 (showing the degree to which the protective cover is bypassed) is obtained by intersecting the I' map with the surface catchment map (Fig. 10).

The surface catchment map was created on the basis of a digital map showing all swallow holes and sinking streams. The 10 m and the 100 m zones were created with the buffer command and the catchments of the sinking streams were delineated automatically from the digital elevation model (DEM).

The *PI vulnerability map*

The final *PI* vulnerability map was obtained by intersecting the *P* and *I* maps (Fig. 12). The protection factor π was calculated by multiplying the *P* and *I* factors. The range of values for π was

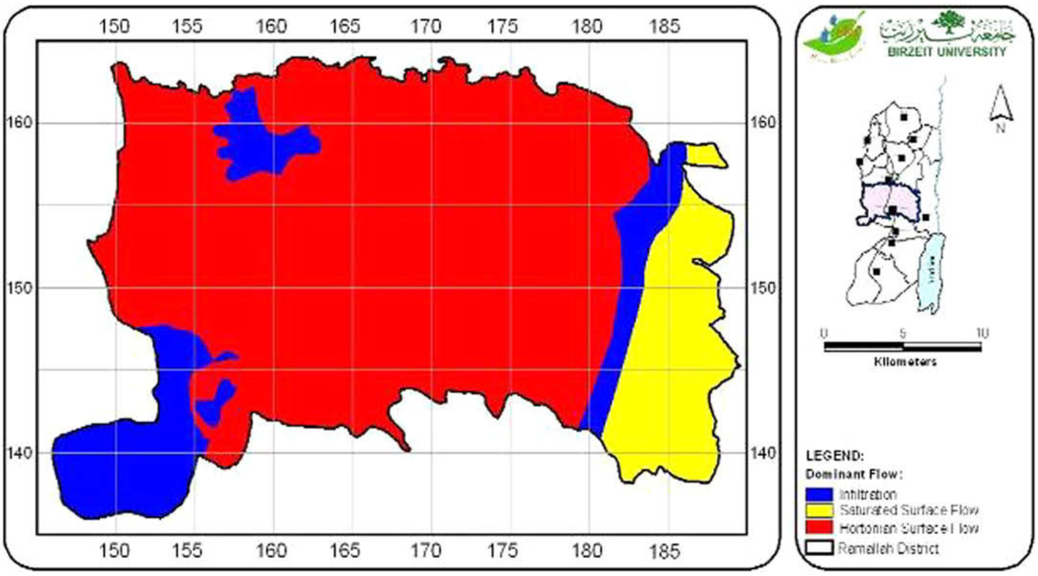

Figure 7. Dominant flow process for each soil type. (For interpretation of the references to colour in this figure legend, the reader is referred to the web version of this article.)

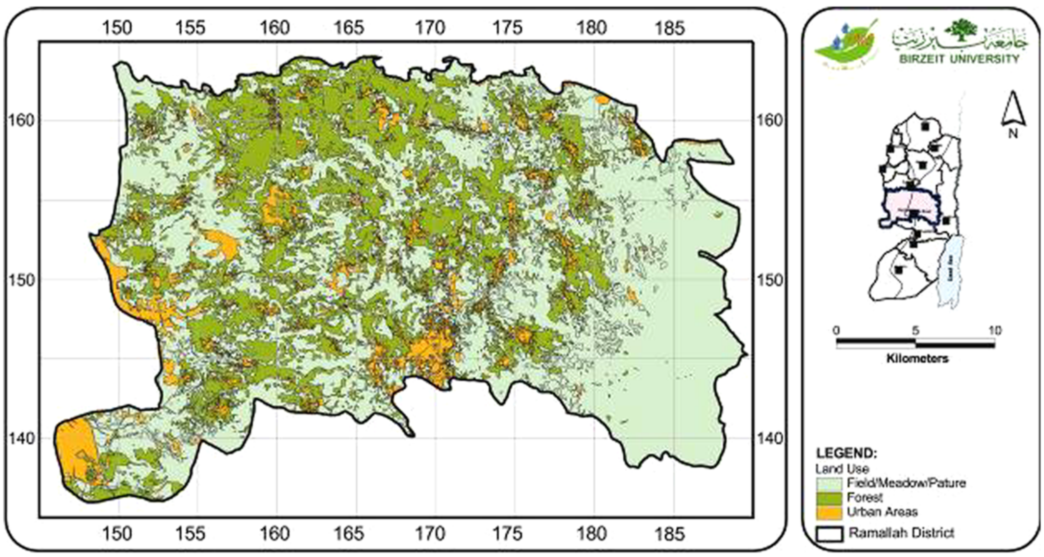

Figure 8. Land use map for Ramallah district. (For interpretation of the references to colour in this figure legend, the reader is referred to the web version of this article.)

Table 10
I' factors for different land use.

Dominant flow type	Slope		
	0–3.5%	3.5–27%	>27%
I' factor for vegetation land use			
Type A	1.0	1.0	1.0
Type D	0.8	0.6	0.4
Type F	0.8	0.4	0.2
I' factor for field/meadow/pasture areas			
Type A	1.0	1.0	1.0
Type D	0.6	0.4	0.2
Type F	0.6	0.2	0.0

subdivided in five classes of natural protection and vulnerability, respectively.

From the final *PI* map, an extreme high to low vulnerability was assigned to the case study area as follows: 5% (41.6 km^2) extreme, 41% (340.7 km^2) high, 31% (257.6 km^2) moderate, 18% (149.6 km^2) low and 5% (41.6 km^2) very low.

Hazard mapping

The majority of the Palestinian communities in Ramallah district especially in rural areas, use cesspits or septic tanks for disposal of wastewater. Wastewater infiltrate from these cesspits to the groundwater. Septic tanks are evacuated by vacuum tankers, the contents of which usually discharge randomly into open land, sewerage networks and irrigation channels.

The wastewater from most factories in Ramallah district has no treatment for the effluent and it is disposed of directly to the sewage and then to the wastewater treatment plants. The industries in the district vary from pharmaceutical, dairy, textile, detergents, soft drink and stone cutting. Quarries and stone cutting represent one of the most important industries in some localities within Ramallah district. They discharge large quantities of slurry into the wadis and dumping sites (UNEP, 2003).

Olives are a very important cultivated product in the West Bank. There are about 26 Olive-mills in Ramallah district. The olive mills start working during the rainy season from October up to December. This increases the risk of groundwater pollution. Most of these

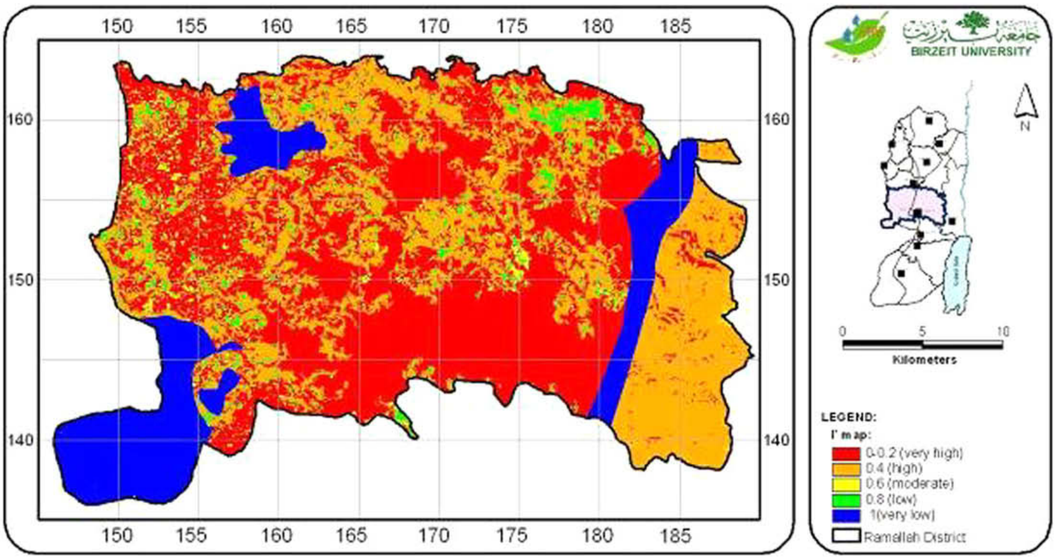

Figure 9. I' map. (For interpretation of the references to colour in this figure legend, the reader is referred to the web version of this article.)

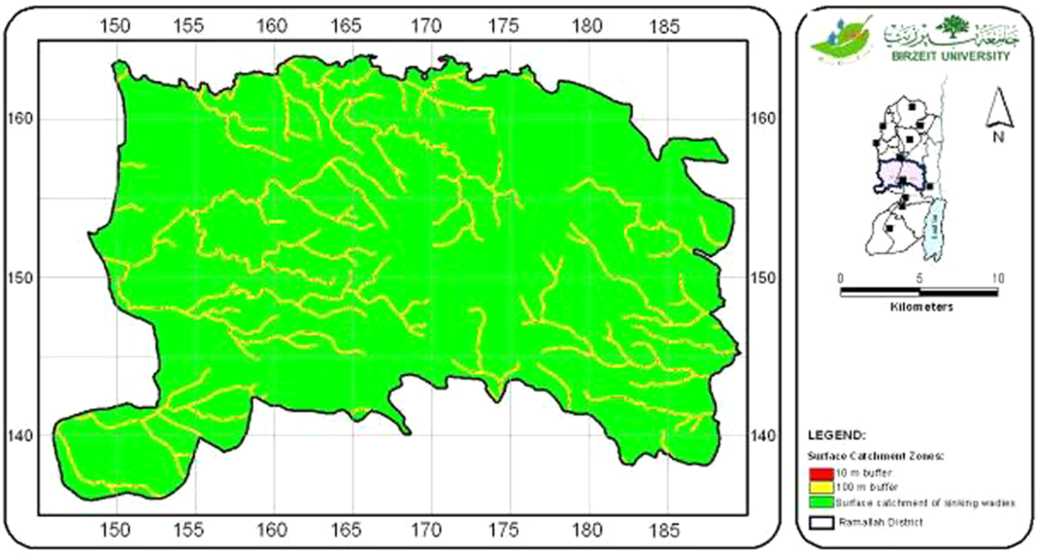

Figure 10. Surface catchment map. (For interpretation of the references to colour in this figure legend, the reader is referred to the web version of this article.)

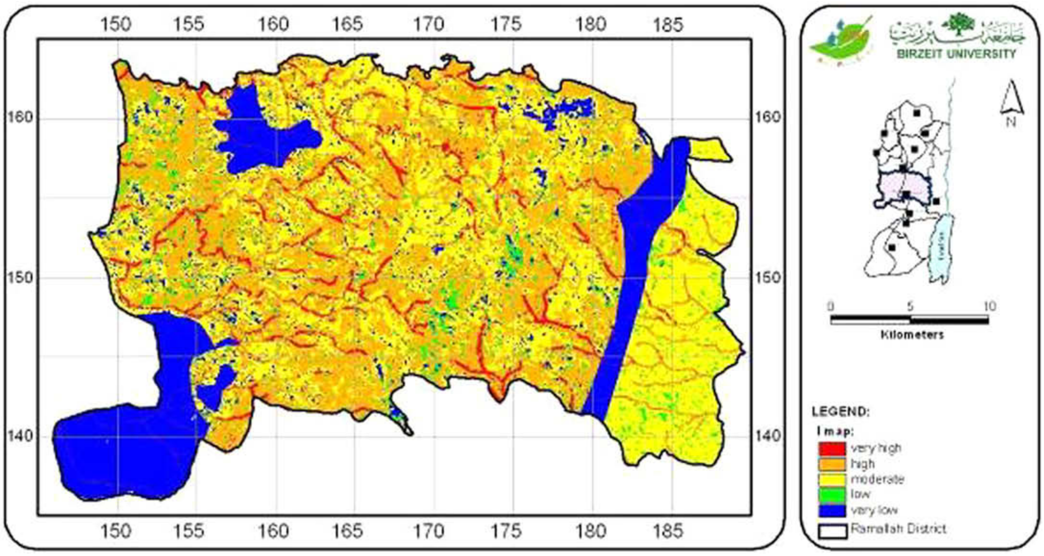

Figure 11. *I* map. (For interpretation of the references to colour in this figure legend, the reader is referred to the web version of this article.)

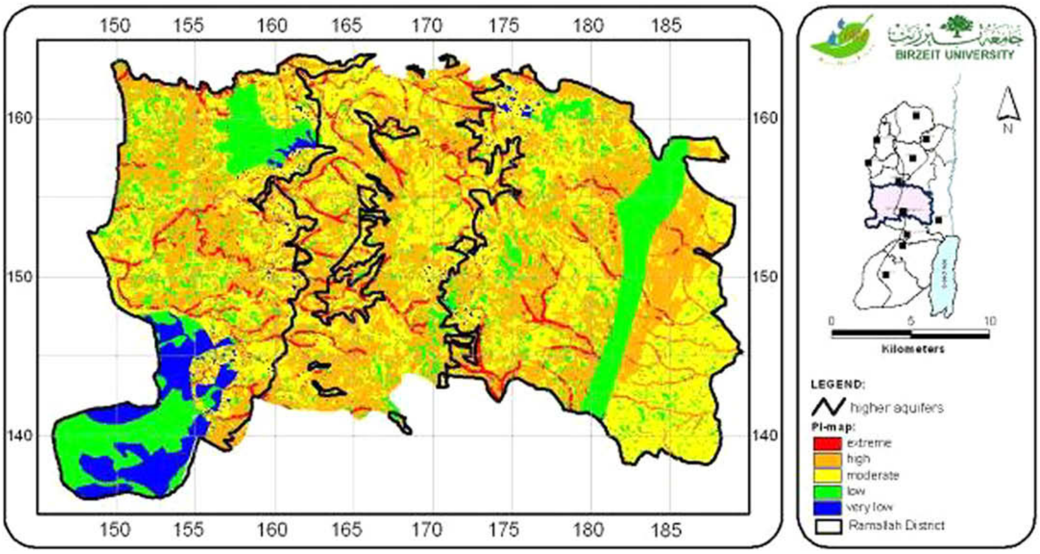

Figure 12. *PI* vulnerability map. (For interpretation of the references to colour in this figure legend, the reader is referred to the web version of this article.)

olive mills discharge their Zebar into the major wadis. The disposal is considered an urgent ecological problem that deteriorates the environment in the Ramallah district.

There are many dumping sites in the district, since each community is surrounded by its own dumping site. Those dumping sites have been chosen in an arbitrary fashion and not well-designed, i.e., no specific concern for groundwater and aquifer contamination. The lack of waste separation implies that hazardous and medical waste disposal is also uncontrolled. Batteries, liquid wastes, and potential hazardous wastes are mixed in with solid (household) wastes. Liquid waste materials are disposed into uncontrolled dumping sites as well as sewers and cesspits (UNEP, 2003).

The hazard mapping for the case study area followed the procedure as proposed by COST Action 620 (Zwahlen, 2003) described earlier. The first step consisted of surveying the infrastructure of the case study area, e.g. villages, sewers and roads. In a second step all the mapped hazards were visited in the field to assess their properties with respect to the quantity of relevant substances and any reduction factor. Further hazards were mapped simultaneously during the fieldwork. Often the required data were unknown and, thus, the ranking factor (Q_n) and the reduction factor (R_f) were estimated on the basis of the relative size and the technical conditions of the hazard.

The following hazards were identified in the case study area: urbanization with leaking sewer pipes and sewer systems; villages without sewer systems; waste water discharge into surface watercourses; garbage dumps; gasoline stations; various industries like pharmaceutical, dairy, textile, detergents, soft drink, quarries and stone cutting.

For data handling and graphical processing the geographical information system (GIS) was used. Within this software, a vector data model with points, lines and polygons was chosen to receive comparable data to the vulnerability map which also consists of vector data. A database consisting of specific layers (covers) was

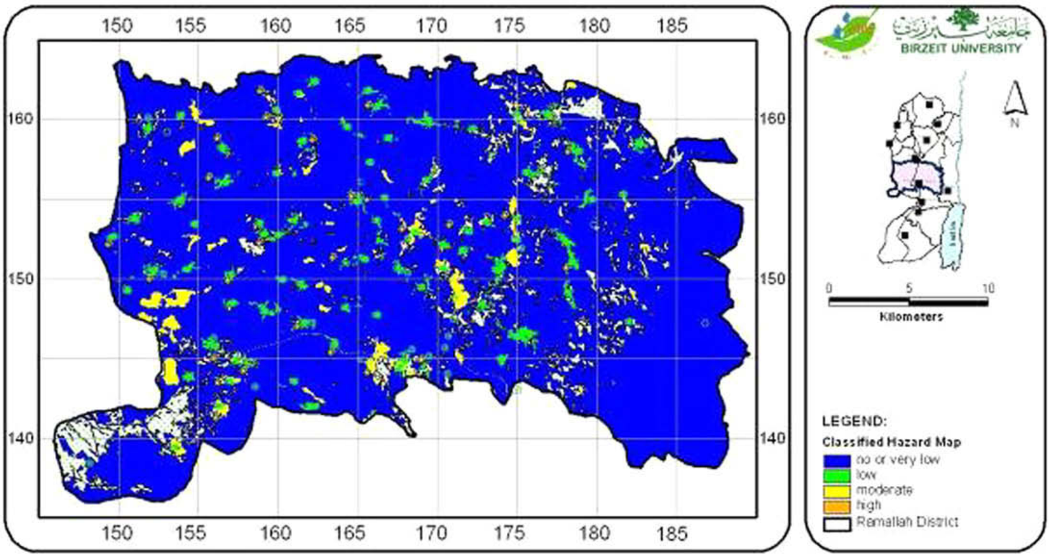

Figure 13. Classified hazard index map for Ramallah district. (For interpretation of the references to colour in this figure legend, the reader is referred to the web version of this article.)

established for each type of hazard taking into account the spatial properties of the hazards.

The weighting (H) which describes the harmfulness of the hazard to the groundwater was determined according to the values proposed by Cost 620 (see Table 2 as an example). The ranking value (Q_n) was assessed considering the range of possible technical specifications of each hazard type which range between 0.8 and 1.2. For example, gasoline stations were ranked according to their size and number of pumps, ranging from single pumps ($Q_n = 0.8$) to highly frequented large gasoline stations ($Q_n = 1.2$). The reduction factor (R_f) considers the probability for a contamination event to occur. If no information is available for such an assessment an R_f-value of one is used. No information was available relating to the probability of a contamination event for any of the mapped hazards.

For the calculation of the Hazard Index (Eq. (1)), all required coefficients (H, Q_n, R_f) were entered in the form of attributes (columns). The Hazard Index was evaluated with a calculating tool available in the GIS and stored as a separate column. The final database thus includes layers (hazard types) with attribute information stored in tables. The columns of these tables contain spatial information and values for H, Q_n, R_f, HI and the hazard index classes. Each row of the table represents one hazard with all the representative data.

The classified map presented in Fig. 13 shows the hazards according to their Hazard Index class representing the hazard level based on Table 3.

The type of hazards and their corresponding degree of harmfulness may partly change in the future because of infrastructure development that is being planned at the moment. Pipes taking the wastewater elsewhere for treatment will enable such treatment within the test site to cease. On the other hand, new industrial factories are planned which will increase the number of hazards.

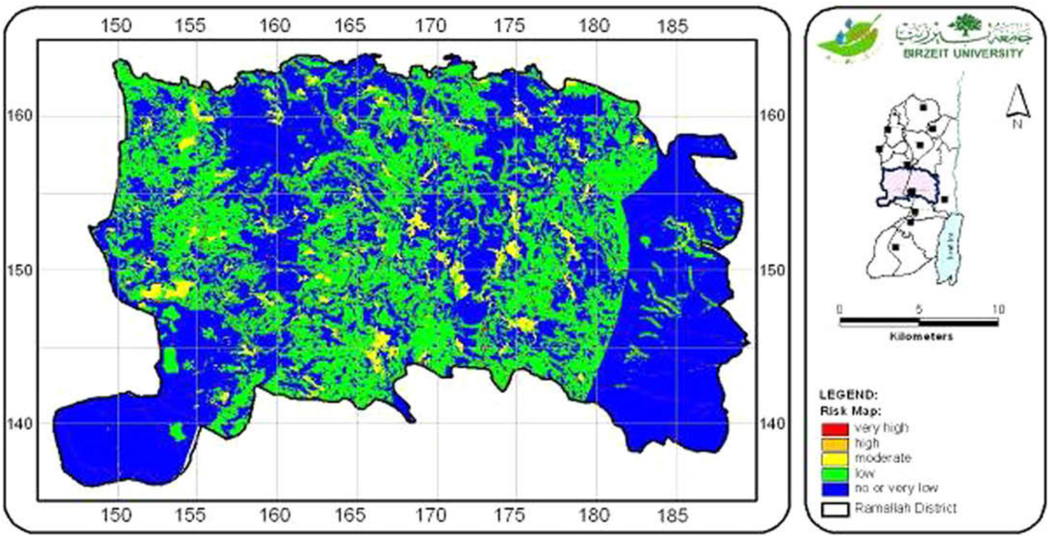

Figure 14. Risk map of Ramallah district. (For interpretation of the references to colour in this figure legend, the reader is referred to the web version of this article.)

Risk mapping

In the risk map of Ramallah district, point hazards kept their original spatial extension whereas linear hazard (roads, sewer wadis) were treated with a 10 m buffer to take into consideration the real spatial dimensions of such objects. The hazard map was converted to a grid map where each cell has its value of (1/HI), then multiplied with the same cell which has its own π-value (Eq. (2)). The risk map was grid map with cell size (50 m × 50 m) as shown in Fig. 14.

Based on Table 4 the risk map of the study area shows that 1% (8.3 km^2) is very high risk, 4% (33.2 km^2) moderate risk, 37% (307.5 km^2) low risk and 58% (482 km^2) very low risk. Hence, almost the entire study area can be classified as low or very low risk area corresponding to the pollution sources.

Discussion

The application of PI method for groundwater vulnerability assessment for Ramallah district has provided a base of information which helps further define the classification system and its potential role in groundwater management. The vulnerability map can assist in the implementation of groundwater management strategies to prevent degradation of groundwater quality.

Large areas in the case study area can be classified as low or very low risk area corresponding to the pollution sources due to the absence of hazards and also due to low vulnerabilities. These areas could consequently be interesting for future development as they are preferable in view of ground water protection. New land use developments can easily be checked for problematical risk levels by constructing potential risk maps, also at a detailed scale, to assess the risk to groundwater contamination of these planned activities.

The case study is a good example of the fact that the final risk map does not include all the information that might be required by an end user. However, to ascertain the risk, which might be posed by future developments, the planner would also require access to the intrinsic vulnerability map and appropriate specific vulnerability maps. As an example, Ramallah municipality is planning to construct a dumping site near Rammon village. The dumping site is a potential source of groundwater contamination. Upon a close view to the vulnerability map, the proposed dumping site is located on a moderate vulnerability area. It is required that new hazard and risk maps be created with the proposed new construction.

Conclusions

Intrinsic vulnerability mapping is not a stand-alone element, but should be integrated into a comprehensive groundwater-protection scheme. COST Action 620 (Zwahlen, 2003) proposes such a scheme, comprising intrinsic vulnerability, hazard and risk mapping for resource and source protection, validation techniques, and hazard and risk assessment.

The proposed COST 620 approach to intrinsic vulnerability, hazard and risk mapping was applied for Ramallah district. The results show that the proposed approach provides a powerful and comprehensive tool for resource and source protection zoning, sustainable groundwater management, installation of monitoring networks, suitable building codes that take account of the vulnerability and value of the groundwater and land use planning.

Finally, classification results should be explored. Maps and summary information could be made available to the public and stakeholders to raise awareness of the resource.

Acknowledgements

The authors wish to acknowledge the help and review provided by numerous researchers, including Dr. Yangxiao Zhou the associate professor in Hydrogeology at UNESCO-IHE. Also, the technical and financial support from PoWER: Jetze Heun, the Director of the partnership for water education and research (PoWER) and Dr Maher Abu-Madi the research coordinator of PoWER.

References

Aller, L., Bennett, T., Lehr, J., Petty, R., 1985. DRASTIC: a standardized system for evaluating ground water pollution potential using hydrogeological settings. US EPA, Robert S. Kerr Environmental Research Laboratory, Ada, OK, EPA/600/2-85/0108, 163pp.

Arkin, Y., 1980. A survey of Karst phenomena, western Judean mountains. Geological survey of Israel, Report MM/5/80, 30pp.

Braun, A.M., 1972. The Keaslon formation in Judea and Shomeron: a model of sedimentation of tidal flats. Israel Geological Society, Annual Meeting, 109pp.

Connell, L.D., Daele, G., 2003. A quantitative approach to aquifer vulnerability mapping. Journal of Hydrology 276, 71–88.

COST 65, 1995. Hydrogeological aspects of groundwater protection in karstic areas. Final report (COST action 65). European Commission, Directorate-General XII Science, Research and Development, Report EUR 16547 EN, Brussels, 446pp.

European Water Directive, 2000. Directive 2000/60/EC of the European parliament and of the council of 23 October 2000 establishing a framework for community action in the field of water policy, European Commission, Brussels.

Foster, S.S.D., 1987. Fundamental concepts in aquifer vulnerability, pollution risk and protection strategy. In: Van Duijevenboden, W., Van Waegeningh, H.G. (Eds.), Vulnerability of Soil and Groundwater to Pollutants, vol. 38. TNO Committee on Hydrogeological Research, Proceedings and Information, The Hague, pp. 69–86.

Gogu, R., Dassargues, A., 2000. Current trends and future challenges in groundwater vulnerability assessment using overly and index methods. Environmental Geology and Water Sciences 39, 549–559.

Goldscheider, N., 2002. Hydrogeology and vulnerability of karst systems: examples from the Northern Alps and Swabian Alb. Ph.D. Thesis, Schr Angew Geol Karlsruhe, Karlsruhe, 236pp.

Goldscheider, N., 2005. Karst groundwater vulnerability mapping: application of a new method in the Swabian Alb, Germany. Hydrogeology Journal 13, 555–564.

Goldscheider, N., Klute, M., Sturm, S.H., 2000. The PI method: a GIS-based approach to mapping groundwater vulnerability with special consideration of karst aquifers. Zeitschrift Fur Angewandte Mathematik Und Mechanik 463, 157–166.

Mimi, Z., Ziara, M., Nigim, H., 2003. Water conservation and its perception in Palestine – a case study. Water and Environmental Management Journal 17, 152–156.

Mimi, Z., Abuhalaweh, O., Wakileh, V., 2004. Evaluation of water losses in distribution networks: Rammallah as a case study. Water Science and Technology: Water Supply 4, 183–189.

Morris, B.L., Foster, S.S.D., 2000. *Cryptosporidium* contamination hazard assessment and risk management for British groundwater sources. Water Science and Technology 41, 67–77.

Morris, B.L., Foster, S.S.D., 1998. *Cryptosporidium* contamination hazard assessment and risk management for British groundwater sources. Water Science and Technology 41, 67–77.

Rofe and Raffety. 1963. West Bank Hydrology, Rofe and Raffety Consulting Engineers. Westminister, London.

Rupert, M.G., 2001. Calibration of the DRASTIC ground water vulnerability mapping method. Ground Water 39 (4), 630–635.

Shachnai, E., 1969. Lower Cretaceous Stratigraphy of the Bet El (Ramallah) mountains. Proceedings of Israel Geology Society 18, 169–170.

SUSMAQ, 2003a. Compiled base data for the numeric flow model of the Western Aquifer Basin, sustainable management of the West Bank & Gaza Aquifers. Palestinian Water Authority and University of Newcastle Upon Tyne, Ramallah, 314pp.

SUSMAQ, 2003b. Hydrogeochemistry of aquifers of the West Bank. Review and interpretation of the available data with regard to recharge, water quality and groundwater flow. Palestinian Water Authority and University of Newcastle Upon Tyne, Ramallah, 60pp.

SUSMAQ, 2004a. Steady state flow model of the Western Aquifer Basin, sustainable management of the West Bank & Gaza Aquifers. Palestinian Water Authority and University of Newcastle Upon Tyne, Ramallah, 174pp.

SUSMAQ, 2004b. Hydrogeological map of the West Bank, 1: 250000 scale, British Geological Survey, University of Newcastle upon Tyne, Palestinian Water Authority.

UNEP, 2003. Desk study on the environment in the occupied Palestinian Territories. United Nations Environment Program, 121pp.

Vrba, J., Zaporozec, A., 1994. Guidebook on mapping groundwater vulnerability, vol. 16. Int Contrib Hydrogeol, Hannover. 131pp.

Zwahlen, F., 2003. Vulnerability and risk mapping for the protection of carbonate (karst) aquifers, final report (COST action 620). European Commission, Directorate-General XII Science, Research and Development, Brussels, 297pp.